Minimizing context-dependency of gene networks using artificial cells

Yunfeng Ding[1], Luis E. Contreras-Llano[1], Eliza Morris, Michelle Mao, Cheemeng Tan*

Department of Biomedical Engineering, University of California Davis, Davis, CA, USA

[1]: These authors contributed equally to this work.

*Correspondence to: cmtan@ucdavis.edu

Abstract

The functioning of synthetic gene circuits depends on their local chemical context defined by the types and concentrations of biomolecules in the surrounding milieu that influence gene transcription and translation. This chemical-context dependence of synthetic gene circuits arises from significant yet unknown crosstalk between engineered components, host cells, and environmental factors, and has been a persistent challenge for synthetic biology. Here, we show that the sensitivity of synthetic gene networks to their extracellular chemical contexts can be minimized and their designed functions rendered robust using artificial cells, which are synthetic biomolecular compartments engineered from the bottom-up using liposomes that encapsulate the gene networks. Our artificial cells detect, interact with, and kill bacteria in simulated external environments with different chemical complexity. Our work enables the engineering of synthetic gene networks with minimal dependency on their extracellular chemical context and creates a new frontier in controlling robustness of synthetic biological systems using bioinspired mechanisms.

Keywords: artificial cells, biomimetics, synthetic gene circuits, molecular crowding, robustness, quorum sensing, antimicrobial

Introduction

Context-dependency of synthetic gene, protein, and metabolic networks is a widely recognized problem in cellular engineering [1]. When inserted into different host cells, synthetic networks may fail to function or exhibit unexpected dynamics if they interact with the host networks through resource competition [2], growth rate modulation [3], culturing environment [4], and titration of regulatory proteins [5]. To resolve the issue of context-dependency, several strategies have been developed to insulate synthetic networks, including insulator sequences that prevent interactions between genetic elements [6-7], insulator modules that separate upstream and downstream networks [7], thermal inducible parts that reduce the temperature dependence of an oscillator [8], and spatial compartmentalization of engineered bacteria [9]. However, the existing strategies cannot buffer synthetic gene networks from their extracellular chemical context, defined by the types and concentrations of molecules surrounding the networks that influence gene transcription and translation.

A plausible way to reduce the extracellular chemical-context dependency of genetic networks is to isolate the network in a physical compartment and focus all energy usage within the network, while tightly controlling the exchange of chemicals at the interface of the compartment. Along this line, artificial cells have been constructed from the bottom up by encapsulating synthetic gene networks and cellular machinery inside liposomes [10-28]. They have been engineered to communicate with natural cells [20, 29-30], separate genetic modules [31], mimic predator-prey interactions [32], inhibit tumor growth[33], function as artificial organelles[34], and serve as protocell models [12, 35]. The artificial cells are often studied using specific extracellular chemical environments to demonstrate their functions, with minimal consideration of their dynamics and the ability to work outside the tested environments, especially without the

extracellular presence of chemicals required for cell-free gene expression. This consideration is non-trivial because it requires control of both synthetic circuits and membranes of artificial cells, which in turn affect stability, production yield, and permeability of artificial cells. Therefore, while it seems plausible that gene expression inside artificial cells should be robust against certain fluctuation of extracellular chemical conditions, yet the features that confer such robustness in artificial cells are unclear. Answers to the question will allow application of synthetic genetic circuits in situations where it is not possible to control the extracellular media.

Here, we demonstrate that artificial cells can sense, react, and interact with bacteria and themselves in extracellular media with different complexity of salts and chemicals that perturb gene expression. We investigate features of artificial cells that confer the minimal dependence on chemical-context. Specifically, we engineer artificial cells that isolate synthetic gene networks in a molecularly crowded milieu, focus energy usage to perform only their designed functions, and control chemical exchange between the networks and the environment, in which the osmotic balance is regulated to assure the viability of bacteria and the functioning of artificial cells. We first minimize the extracellular chemical-context dependence of artificial cells by exploiting lipid composition, membrane permeability, and molecular crowding (Figure 1). Different extracellular chemical context is simulated using water, a universal buffer, and a nutrient-rich medium, representing environments with increasing complexity of molecular composition. Next, we show robust communication between artificial cells and bacteria through quorum-sensing regardless of the extracellular chemical context (Figure 2&3). We also show artificial cells that detect quorum-sensing signals in biofilms, corroborating their ability to work in different spatial contexts (biofilm *vs* planktonic) (Figure 4). Finally, we demonstrate a complex feedback response in which artificial cells function as nano-liter systems that both detect and kill bacteria with

minimal dependency on their extracellular chemical context (Figure 5). Our work provides a novel approach that buffers synthetic biological networks from their extracellular chemical context using artificial cells, opening the door toward using artificial cells as nanofactories [36] and biosensors [37].

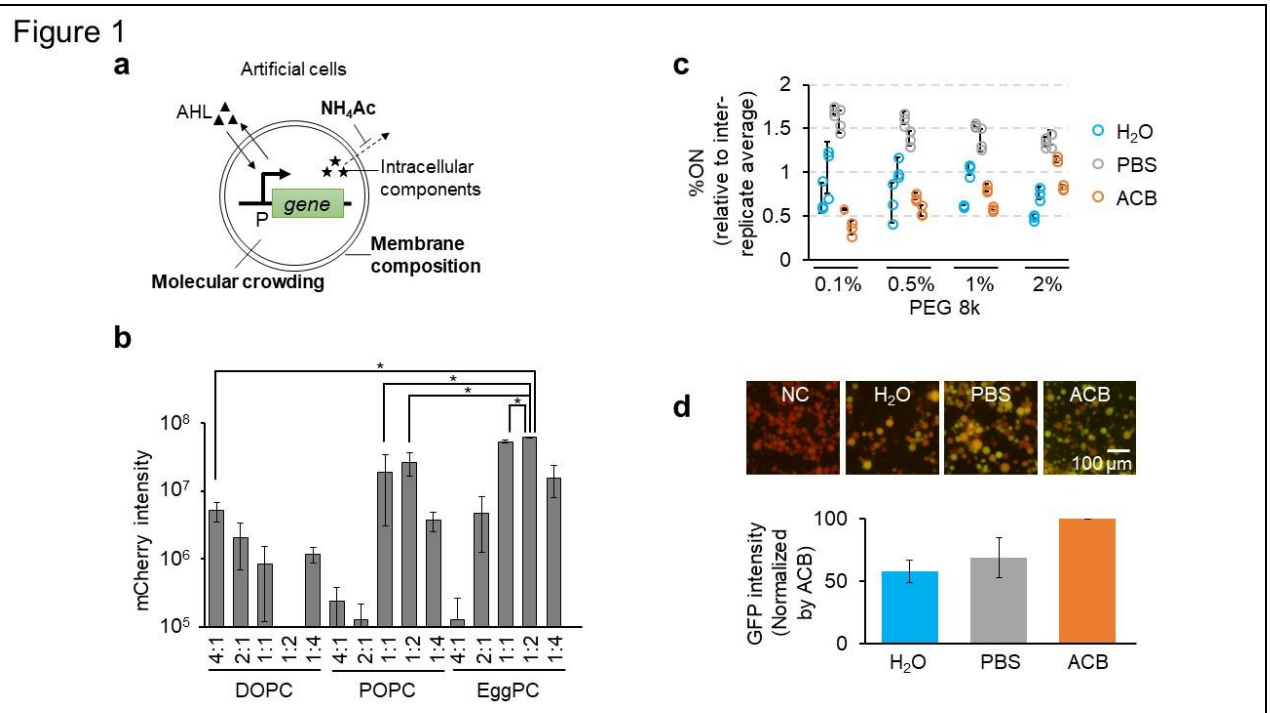

Figure 1: Minimal chemical-context dependency of gene expression in artificial cells.

a, Extracellular chemical-context dependency of artificial cells is reduced by optimizing membrane composition, incorporating molecular crowding that increases the robustness of gene expression, and controlling external environment that modulates the osmotic balance of artificial cells.

b, The yield of artificial cells prepared from different lipid composition. We test different ratios between phospholipids (DOPC, POPC, EggPC) and cholesterol. Artificial cells are labeled by purified mCherry and measured by a fluorescence microscope. The yield of artificial cells is

reflected by mCherry intensity. The highest yield is obtained using EggPC:Cholesterol=1:2 which results in an average of 10^6 artificial cells/ml, (Standard two-tail t-test $*P \leq 0.005$). Each error bar represents s.d. (n=6).

c, Crowding agent reduces the fluctuation of %ON across different external chemical environments. Artificial cells contain different weight/volume percentage of PEG8k. Artificial cells containing pIVEX-(P_{T7})-GFP are incubated in H_2O, PBS, and artificial cell buffer. GFP intensity is recorded using a fluorescence microscope and analyzed as described in Supplementary Materials and Methods, Sections *M.5&M.6*. 2% PEG exhibits the lowest fluctuation in %ON across the three different conditions tested and between technical replicates. Two biological replicates for H_2O (blue circles), PBS (grey circles) and ACB (orange circles), each with three technical replicates, are shown. Each error bar represents s.d. (n=3).

d, Changes of GFP expression in artificial cells across different extracellular chemical environments. Artificial cells expressing GFP are incubated in H_2O, PBS, and artificial cell buffer. GFP expression level is recorded by microscopy (top panels), and flow cytometry (bottom panel) after 5 h incubation at 37°C. (Scale bar for artificial cells = 100 μm). Each error bar represents s.d. (n=6).

Results

Engineering artificial cells to buffer gene networks from the extracellular chemical context

We first investigate design principles that reduce the extracellular chemical-context dependency of artificial cells (Figure 1a). In this study, we focus on binary response and short operating duration (<5 hours) of the synthetic bacteria and artificial cells in the context of their common functions as biosensors or transient drug-screening and delivery devices. We note that

artificial cells are not currently feasible as the replacement of living cells for applications that require continuous protein synthesis for extended periods of time (>5 hours) due to the limited availability of resources inside the artificial cells.

Membrane composition governs the assembly process, permeability, and stability of artificial cells. Previous work has used freeze-dry and rehydration methods to form artificial cells [17, 20, 29], which invariably produce multi-lamellar membranes [38-39] that impact permeability and increase heterogeneity of artificial cells. Instead, we use the water-in-oil emulsion transfer method to construct unilamellar artificial cells (the membrane of artificial cells is labeled using 0.5% of DOPE-Rhodamine B) that constitutively express a reporter green fluorescent protein (GFP) from a P_{T7} promoter (pIVEX-(P_{T7})-GFP) (Figure S1a). Furthermore, it is now well-established that cholesterol affects membrane fluidity and stability [40]. Along this line, we examine the effect of lipid composition on the yield of artificial cells by varying the ratio between different phospholipids and cholesterol. We find that Egg Phosphatidylcholine:Cholesterol (EggPC:Chol)=1:2 gives rise to the highest yield of artificial cells by measuring mCherry encapsulated inside the cells. With this lipid composition, we achieved an average of 10^6 artificial cells/ml, each with a diameter of 10-50 μm (Figure 1b and Figure S1b). Additional results show that the use of 1-palmitoyl-2-oleoyl-sn-glycero-3-phosphocholine (POPC) in the construction of artificial cells results in a slightly higher level of GFP expression compared with those constructed using Egg PC (Figure S3). Here, we decided to prioritize the yield of AC over the absolute GFP expression level. Therefore, for subsequent experiments, we construct artificial cells using the water-in-oil transfer method and a membrane composition of EggPC:Chol=1:2, which generates the highest number of artificial cells with unilamellar membranes.

The encapsulation of transcription-translation machinery, cofactors, and other molecules required for robust protein synthesis naturally creates conditions for osmotic imbalance due to the differences in concentration, size, and polarity of the molecules present inside artificial cells. Therefore, a highly permeable membrane diminishes transcription-translation ability of artificial cells because encapsulated chemical components, such as amino acids, cofactors, ions, and other small molecules essential for protein synthesis can diffuse out to equilibrate with the external environment, resulting in the loss of artificial-cell functions. To achieve osmotic balance, we first prepare a set of artificial cell buffers missing single component of the buffer and incubate artificial cells in these buffers. We assume that the missing component in the external environment may cause the loss of critical factors involved in transcription-translation through passive out-diffusion, diminishing gene expression activities inside artificial cells. Based on this assay, we find that ammonium acetate (NH_4Ac) alone is sufficient to maintain GFP (pIVEX-(P_{T7})-GFP) expression in artificial cells (Figure S4), likely by equilibrating osmotic balance across the artificial cell membranes. We note that supplementation of ammonium acetate also helps to reduce the fluctuation of ammonium-acetate concentration inside artificial cells, which has been shown to significantly perturb gene expression rates[17]. We also rule out any artifacts due to chemical influence on fluorescence of GFP by showing that the GFP intensity indeed reflects the amount of GFP inside artificial cells (Figure S4e).

In addition, we investigate if the intracellular content of artificial cells may reduce their dependency on extracellular chemical context. Our previous work has demonstrated that molecular crowding reduces the sensitivity of gene expression to chemical perturbation in a cell-free system [17]. Based on the results of this work, we study the effect of a crowding agent on gene expression in artificial cells. Artificial cells containing a different concentration of poly-ethylene

glycol (PEG 8000 Da) are incubated in autoclaved water (H_2O), phosphate buffered saline (PBS), and artificial cell buffer (ACB). All the different buffers contain sucrose and NH_4Ac that are used to regulate osmotic pressure among the different media. H_2O serves as the surrogate of a chemical environment with the minimal components to maintain natural and artificial cell functioning; PBS represents a slightly more chemically complex buffer, being a balanced salt solution that is widely used in biological research; ACB is a chemically complex buffer that contains 35 components, which are the same as the intracellular content of artificial cells. GFP expression levels of the artificial cells are then compared among these three incubation conditions with increasing PEG concentrations. We find that GFP (pIVEX-(P_{T7})-GFP) expression in artificial cells exhibits a reduction in the fluctuation of GFP expression level across the three different external environments (Figure 1c) and a decreasing coefficient of variance with increasing weight/volume percentage of PEG (Figure S5). This result suggests that high concentration of PEG increases the robustness of GFP expression in artificial cells across these widely different external chemical environments. Given these results, 2% (w/v) PEG is used throughout all subsequent experiments.

Finally, we combine the assembly method, membrane composition, and molecular crowding to control gene expression inside of artificial cells. We test GFP (pIVEX-(P_{T7})-GFP) expression in the same three media used in the previous experiment. We find that artificial cells express ~60% of GFP in H_2O, and PBS when compared to GFP levels in ACB (Figure 1d). Here, artificial cells work in all the tested environments because they utilize nearly all energy sources for expressing the target genetic circuits. This compartmentalization of the reaction systems enhances gene expression robustness through molecular crowding and helps to control chemical exchange at their interface with environments. These features are incorporated into artificial cells

to achieve consistent interactions and feedback responses in different extracellular chemical contexts.

Engineering a minimal communication circuit in artificial cells

To demonstrate buffering of the synthetic gene networks from extracellular chemical contexts, we first engineer a minimal quorum-sensing circuit in artificial cells because such circuits challenge the ability of artificial cells in buffering against chemical-context while maintaining communication with external environments. The negative regulatory mode of the promoter is chosen to reduce leaky expression and enhance the sensitivity of the promoter to N-(3-oxohexanoyl)-L-homoserine lactone (AHL). In contrast to previous work that has implemented similar communication circuits in either water droplets [30] or artificial cells [29], we aim to demonstrate the consistent operation of the circuits in different chemical and spatial contexts, as well as embedding of the circuits in feedback response systems.

We first engineer synthetic circuits that consist of a sender module and a receiver module. The sender circuit consists of EsaI that synthesizes AHL in both bacterial cytoplasm and artificial cells (Figure 2a-c). The receiver circuit consists of a novel hybrid promoter $P_{T7\text{-}EsaR}$ designed in this study (Figure 2d-f and Figure S6). Four variants of $P_{T7\text{-}EsaR}$ promoter with different O_{EsaR} sequences are inserted into the plasmid pIVEX-($P_{T7\text{-}EsaR}$)-GFP, in which GFP is expressed as the reporter protein from the $P_{T7\text{-}EsaR}$ promoter. EsaR (derived from *Erwinia Stewartii*) [41] binds to O_{EsaR}, and inhibits gene expression from the hybrid $P_{T7\text{-}EsaR}$ promoter. AHL synthesized by the sender circuit binds to EsaR and causes the release of EsaR from O_{EsaR} (Figure 2g&h). All primers used for plasmid construction are listed in Table S1. pIVEX-($P_{T7\text{-}EsaR}$)-GFP-1 and pIVEX-($P_{T7\text{-}EsaR}$)-GFP-2 exhibit the highest fold change in GFP expression when AHL is added in the cell-free system and bacteria respectively (Figure S6b&c). Therefore,

we use pIVEX-($P_{T7\text{-}EsaR}$)-GFP-1 in artificial cells and pIVEX-($P_{T7\text{-}EsaR}$)-GFP-2 in bacteria for our subsequent study.

To test the performance of the constructed modules, we encapsulate pIVEX-($P_{T7\text{-}EsaR}$)-GFP-1 (variant 1 of the pIVEX-($P_{T7\text{-}EsaR}$)-GFP), EsaI, and the bacterial extract containing both T7 RNA Polymerase and EsaR inside artificial cells. We also ensure that purified EsaI does not contain remnants of AHL from bacteria (Figure S7a-d & f). In the presence of both EsaI (+EsaR +EsaI), artificial cells exhibit higher GFP expression levels than without EsaI (+EsaR -EsaI) (Figure 2h & Figure S7e). GFP expression is inhibited by EsaR and recovered by AHL in bacteria and artificial cells (Figure 2e & Figure S8). Artificial cells carrying pIVEX-($P_{T7\text{-}EsaR}$)-GFP-1 exhibit sensitivity to AHL with K_d=5 nM, while bacteria with pIVEX-($P_{T7\text{-}EsaR}$)-GFP-2 (variant 2 of the pIVEX-($P_{T7\text{-}EsaR}$)-GFP) exhibit K_d=15 nM (Figure 2f). Here, we have demonstrated that artificial cells are able to synthesize and secrete AHL and respond to AHL by expressing GFP. We also show that the artificial cells have high sensitivity to AHL (Figure 2f) and high production rate of AHL (Figure 2b&c). This result represents a fundamental advancement beyond previous work that only demonstrated the functionality of artificial cells [13, 20, 29, 42], but did not measure and control the kinetics of artificial cells. We demonstrate the ability to create artificial cells that mimic both functions and activity of natural cells.

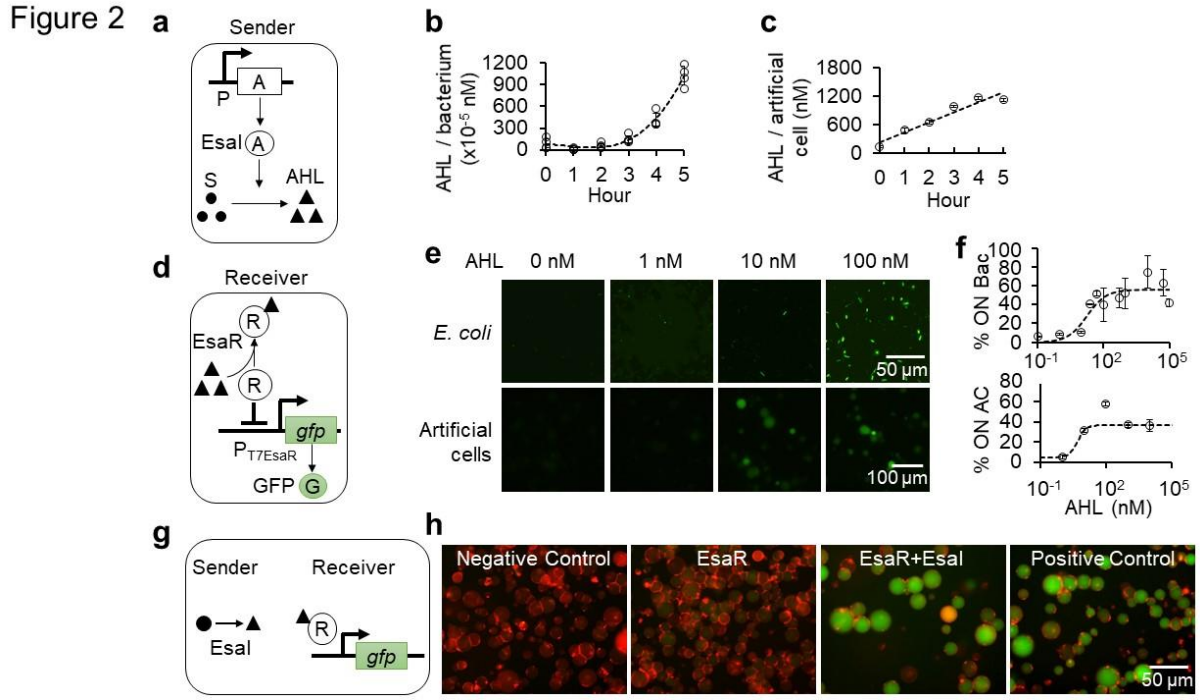

Figure 2: Bottom-up construction and measurement of communication circuits in bacteria and artificial cells.

a, A sender module and a receiver module are engineered to facilitate communication between artificial and natural cells. The sender module contains EsaI that produces the quorum sensing molecule AHL. Black circle represents substrate of AHL. Black triangle represents AHL. "A" represents EsaI.

b, Amount of AHL generated per bacterium in artificial cell buffer over five hours. Each error bar represents s.d. (n=4).

c, Amount of AHL generated per artificial cell without hemolysin (Hem) pores in artificial cell buffer. Each error bar represents s.d. (n=5).

d, The receiver module contains a promoter that is activated by AHL from the sender module. Black triangle represents AHL. "R" represents EsaR.

e, Response of bacteria and artificial cells to different AHL concentrations. Bacteria (upper panel) or artificial cells (lower panel) are incubated with different concentrations of AHL. For both bacteria and artificial cells, 100 nM AHL is sufficient to remove EsaR inhibition and activate GFP expression. Images are taken after 5 h incubation at 37°C. (Scale bar for bacteria = 50 μm). (Scale bar for artificial cells = 100 μm). See replicate images in Figure S8.

f, %ON bacteria (top) and artificial cells (bottom) expressing GFP as a function of AHL concentration. The data are used to construct a mathematical model of the system. Refer to Supplementary Results, Section *R.2* and Supplementary Materials and Methods, Section *M.9* for details on the mathematical model. Each error bar represents s.d. (n=5).

g, Both the sender and receiver modules are included in artificial cells. EsaR binds to $P_{T7\text{-}EsaR}$ and inhibits GFP transcription by T7RNAP. AHL produced in sender cells binds to EsaR in receiver cells. The AHL-EsaR complex is released from $P_{T7\text{-}EsaR}$ and facilitates GFP expression by T7 RNA Polymerase. Black circle represents substrate of AHL. Black triangle represents AHL. "R" represents EsaR.

h, Images of GFP expression in artificial cells (AC). In AC without plasmid (Negative control) and AC without EsaI (EsaR), GFP level is negligible (EsaR). In AC with both EsaR and EsaI (+EsaR +EsaI), GFP level is high (EsaR+EsaI). In AC with EsaR and 10 μM AHL, strong GFP expression is observed (Positive Control). Red fluorescence channel: artificial cell membrane is labeled by 0.5% of DOPE-Rhodamine B (Scale bar for bacteria = 50 μm). Green fluorescence channel: GFP. See replicate images in Figure S7e.

Dotted lines in b, c, and f indicate trend lines.

The communication circuit between artificial cells and bacteria operate with minimal dependency on its extracellular chemical context

The kinetics of artificial cells are critical for the control of their dynamics in cell-cell communication. To understand the kinetics, we build a mathematical model that simulates both the sender and receiver circuits (Eq. S1-S4). We first experimentally measure several key parameters of the synthetic circuits in artificial cell buffer (Table S2). AHL generated by a known number of either artificial cells or bacteria is introduced to a bacterial standard in order to determine their rate of AHL production (Figure 2b&c). The GFP production by both bacteria and artificial cells in response to specific levels of AHL is quantified by fluorescence imaging (Figure 2f). These production rates are used as input parameters in a mathematical model to describe three communication scenarios: artificial cells signaling bacteria, bacteria signaling artificial cells, and sender artificial cells signaling receiver artificial cells (refer to Supplementary Results, Section *R.2* and Supplementary Materials and Methods, Section *M.9*).

Based on the model and the quorum-sensing circuit, we first investigate one-way communication from artificial cells to bacteria in only artificial cell buffer because the receiver bacteria do not work in H_2O and PBS. Sender artificial cells containing EsaI are tagged with mCherry and co-incubated with bacterial strain BL21AI containing EsaR and pIVEX-($P_{T7\text{-}EsaR}$)-GFP-2. Sender artificial cells synthesize AHL, which then trigger GFP expression in the bacteria. As a negative control, artificial cells without EsaI do not activate GFP expression in the receiver bacteria. To quantify the sensitivity of receiver bacteria to artificial sender cells, we test bacterial response with different amounts of artificial cells. Flow cytometry results show that bacteria start to respond to 0.05 µl (an estimate of 50 artificial cells) of sender artificial cells (Figure 3a & Figure S9). The results of this set of experiments are given in %ON of cells, and we define the "ON &

OFF" state of GFP producing cells based on fluorescence intensities quantified at a pixel level using microscopy images, or at the cell level in flow cytometry as described in detail in Supplementary Materials and Methods, Sections *M.5*&*M.6* and in Figure S2. We consider that for future applications of artificial cells as biosensors, a binary response will be preferred over fluorescence intensity representation. Furthermore, analysis of the data as either %ON or absolute intensity does not affect interpretation of the results (e.g., Figure S9b&d, Figure S10b&d & Figure S11b&d). The model predicts that the %ON (with GFP expression) of bacterial cells is 33% at high AHL levels, while the experimentally observed %ON of bacterial cells is 30% (Figure 3b). The result is also consistent with GFP intensity data from flow cytometry measurement (Figure S9d). Real-time experiments (Video S1) suggest that the dynamics of the system are governed primarily by intact artificial cells. The results show that the communication circuits between bacteria and artificial cells work as designed.

To demonstrate the robust functioning of artificial cells in different extracellular chemical contexts, we investigate one-way communication from bacteria to artificial cells in H_2O, PBS, and artificial cell buffer, all containing sucrose and NH_4Ac. Specifically, sender bacteria carry a plasmid pIVEX-(P_{T7})-EsaI that expresses EsaI constitutively. Receiver artificial cells contain EsaR and $P_{T7\text{-}EsaR}$-GFP-1 and are tagged with mCherry. The results show that the sender bacteria produce AHL, which activates GFP expression in artificial cells under all tested extracellular chemical contexts. Without pIVEX-(P_{T7})-EsaI, sender bacteria cannot produce AHL and fail to communicate with the receiver artificial cells (Figure 3c & Figure S10). In this case, our model predicts a %ON for artificial cells of 32% in artificial cell buffer, which closely matches the experimentally observed %ON of artificial cells of 34% (Figure 3d). The result is also consistent with the GFP intensity data from flow cytometry measurement (Figure S10d). The artificial cells

also respond with a similar trend to the sender bacteria in all tested extracellular chemical contexts. These experiments establish artificial cells as biosensors of bacterial quorum-sensing molecules in different extracellular chemical contexts.

Figure 3

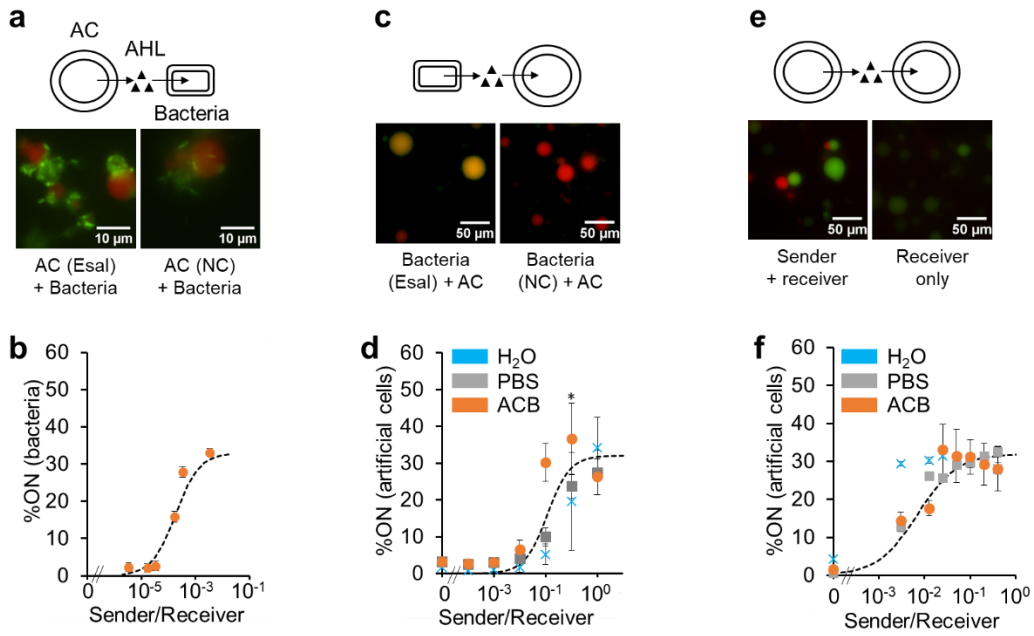

Figure 3: Unidirectional communication between artificial cells and natural cells in different extracellular chemical contexts.

a, Artificial cells signaling bacteria in artificial cell buffer. Artificial cells with (EsaI) or without EsaI (NC) are constructed and incubated with BL21-AI containing the receiver module (pAC-EsaR and pIVEX-($P_{T7\text{-}EsaR}$)-GFP-2). Bacteria exhibit a higher GFP expression level when incubated with artificial cells containing EsaI than with negative-control artificial cells. Images are taken after incubating the cells in artificial cell buffer at 37°C for 5 h. (Scale bars = 10 μm). See replicate images and flow cytometry results in Figure S9.

b, Response of bacteria to ratios between senders and receivers in artificial cell buffer. Each error bar represents s.d. (n=6).

c, Bacteria signaling artificial cells. Bacteria with (EsaI) or without pIVEX-(P_{T7})-EsaI (NC) are mixed with artificial cells containing the receiver module (EsaR and pIVEX-($P_{T7\text{-}EsaR}$)-GFP-1) and labeled with mCherry. Artificial cells exhibit higher GFP expression levels when incubated with bacteria containing pIVEX-(P_{T7})-EsaI (that expresses EsaI) than with negative control artificial cells. Images are taken after incubating the cells in artificial cell buffer at 37°C for 5 h. (Scale bars = 50 μm). See additional images in other incubation buffers and flow cytometry results in Figure S10.

d, Response of artificial cells to ratios between senders and receivers in H_2O (Blue), PBS (Gray), and artificial cell buffer (Orange). Each error bar represents s.d. (n=6). Standard two-tail t-test *P $\leq$ 0.05.

e, Sender artificial cells signaling receiver artificial cells. Sender cells labeled with mCherry and containing 0.3 nM EsaI are incubated with receiver cells containing the receiver module (pIVEX-($P_{T7\text{-}EsaR}$)-GFP-1). The negative control group consists of only receiver artificial cells. Receiver cells have a higher GFP expression level when incubated with sender artificial cells than with the negative control. Images are taken after incubating the cells in artificial cell buffer at 37°C for 5 h. (Scale bar = 50 μm). See additional images in other incubation buffers and flow cytometry result in Figure S11.

f, Response of artificial cells to ratios between senders and receivers in H_2O (Blue), PBS (Gray), and artificial cell buffer (Orange). Each error bar represents s.d. (n=6).

(b, d, f) The %ON of bacteria and artificial cells is calculated from images (Solid markers) as described in Supplementary Materials and Methods, Section *M.6* and in Figure S2. Experimental

results from artificial cell buffer (Orange circles) match the corresponding model results (Dashed line).

In addition, we study communication between artificial cells in H_2O, PBS, and artificial cell buffer. Sender artificial cells containing EsaI are labeled with mCherry. They produce AHL, which subsequently induces GFP expression in receiver artificial cells that contain EsaR and pIVEX-($P_{T7\text{-}EsaR}$)-GFP-1. In contrast, without the sender artificial cells, the receiver artificial cells only exhibit basal GFP expression levels (Figure 3e & Figure S11). Our model again predicts a %ON for artificial cells of 32% at saturating AHL concentrations in artificial cell buffer, closely matching the experimentally observed %ON for artificial cells of roughly 30% (Figure 3f). As in the previous two experiments, this result closely matches the GFP intensity data from flow cytometry measurement (Figure S11d). The results also show that the artificial cells communicate with similar sensitivity toward sender/receiver ratio in the three chemical environments. Through these results, we have established, for the first time, three unidirectional communication modes between artificial cells and bacteria using the same modular cellular parts in different extracellular chemical contexts. Due to the minimal chemical-context dependency of artificial cells, genetic networks inside artificial cells give rise to similar dynamics in the three environments, without requiring any changes in the networks to accommodate the different chemical conditions. In addition, our mathematical model allows us to predict the results of one-way communication experiments in all conditions tested, and to interpret any potential variation of artificial-cell functions in different environments.

Figure 4

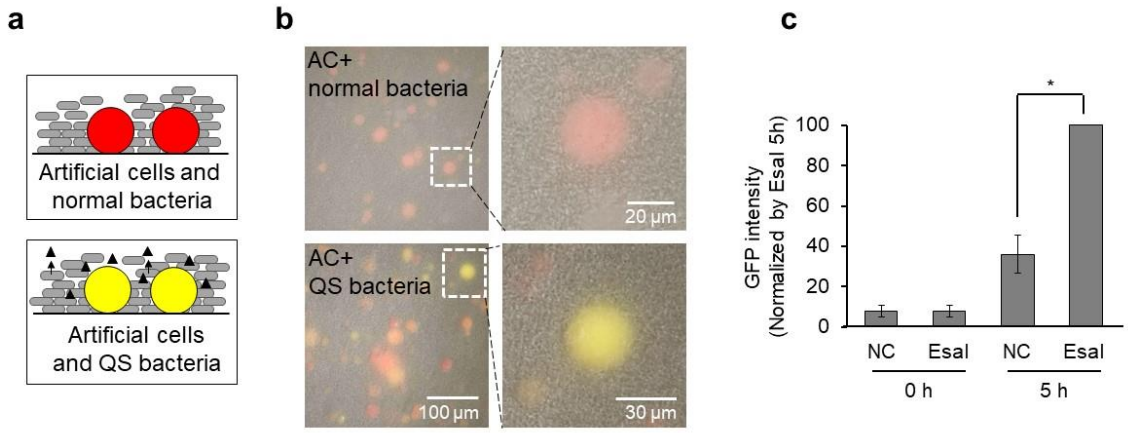

Figure 4: Artificial cells as biosensors of quorum-sensing signals in crowded bacterial environment.

a, Schematic illustration of artificial cells as biosensors in biofilm. Artificial cells are labelled by mCherry. When incubated with bacteria that synthesize AHL, artificial cells express GFP. Red circle: artificial cells labeled with mCherry. Yellow circle: artificial cells labeled with mCherry, and express GFP. Gray rod: bacteria. Black triangle: AHL.

b, Artificial cells containing pIVEX-(PT7-EsaR)-GFP-1 are prepared as described in Methods. 500 µl overnight culture of bacteria are washed and incubated with artificial cells in 35 µl H_2O. Images are recorded after incubating cells in H_2O at 37°C for 5 h. (Scale bar = 100 µm).

c, Flow cytometry data of extracted artificial cells from (**b**). Artificial cells exhibit significantly higher GFP intensity when they are incubated with bacteria containing EsaI than non-modified bacteria (NC). (Standard two-tail t-test $*P \leq 0.005$). Each error bar represents s.d. (n=6). GFP intensities are normalized by "EsaI 5 h" intensity, s.d are then calculated, and the mean values are plotted.

The reliable functioning of the artificial cells in different extracellular chemical contexts establishes a route toward using the artificial cells as biosensors of quorum-sensing signals inside a biofilm that is typically nutrient deprived [43]. Unlike the previous experiments using planktonic cells (Figure 1-3), this application requires artificial cells that both maintain functions of synthetic gene networks and remain stable among crowded bacteria. Artificial cells carrying receiver circuits are embedded inside a biofilm that contains either normal bacteria or sender bacteria (Figure 4a). The biofilm is established in H_2O to mimic an extreme case of nutrient-deprived environments. To form a biofilm, an overnight culture of bacteria is concentrated ten times and incubated with artificial cells in a static culture chamber. Indeed, both microscopy (Figure 4b) and flow cytometry (Figure 4c) results show that the receiver artificial cells generate stronger fluorescence signals in the presence of sender bacteria than in the presence of normal bacteria. The results highlight the buffering of synthetic gene networks from both chemical (H_2O, PBS, artificial cell buffer) and spatial contexts (biofilm *vs.* planktonic) using the artificial cells.

Buffering feedback response between artificial cells and bacteria from the extracellular chemical context

To demonstrate further the ability of artificial cells in buffering gene networks from extracellular chemical context, artificial cells should be capable of feedback response with natural cells in different extracellular chemical contexts, acting as both senders and receivers. Therefore, we extend the genetic modules to enable feedback responses between artificial cells and bacteria. We focus on negative feedback responses through antimicrobial peptides (APs) that allow dynamic adaptation of a system in response to environmental stimuli. Specifically, we replace the reporter gene GFP in either artificial cells or bacteria with an AP that lyses both bacteria and artificial cells

(Figure 5a-c). Based on the characterization of two different APs (refer to Supplementary Results, Section *R.3*, and Figure S12), we implement negative feedback responses between artificial cells and bacteria using a synthetic AP, Bac2A [44].

Figure 5

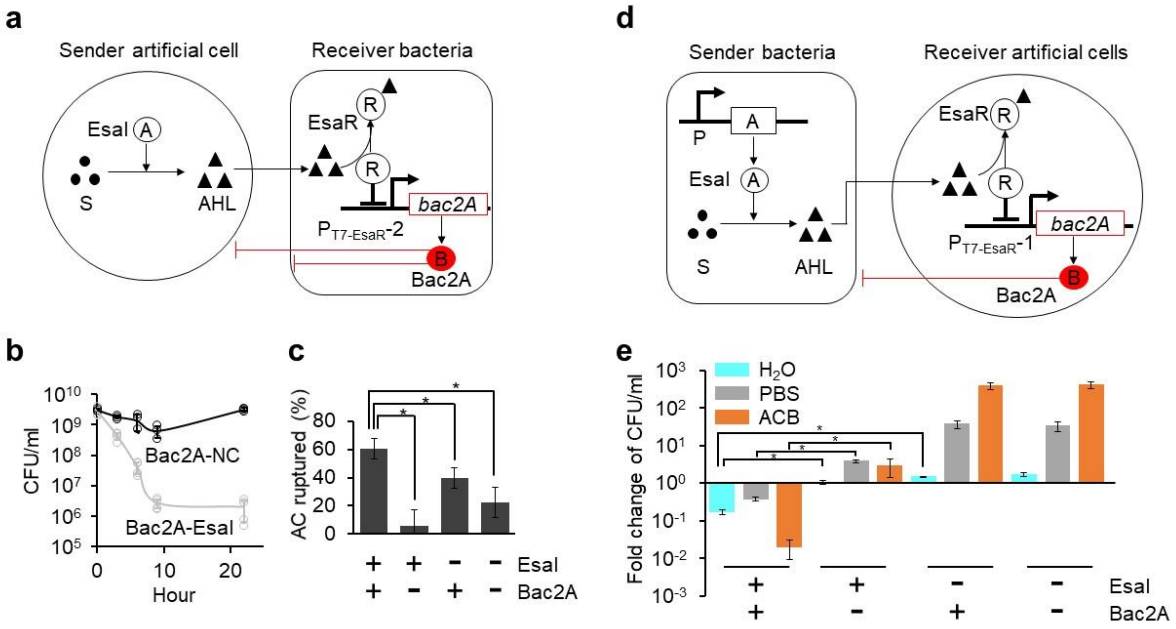

Figure 5: Negative feedback responses between artificial cells and bacteria.

a, The schematic illustrates a negative feedback response between artificial cells and bacteria. AHL produced by EsaI in artificial cells is detected by bacteria. The bacteria express Bac2A, kill themselves, and then rupture artificial cells, thus completing the negative feedback response. "A" represents EsaI, "S" represents substrates of EsaI, and "R" represents EsaR.

b, CFU of bacteria through the negative feedback response (**a**) in the artificial cell buffer. Artificial cells are mixed with bacteria containing pAC-EsaR (expresses EsaR) and pIVEX-($P_{T7\text{-}EsaR}$)-Bac2A (expresses Bac2A from the $P_{T7\text{-}EsaR}$ promoter) and incubated at 37°C. CFU analysis shows that the

density of bacteria decreases when incubated with artificial cells containing EsaI, as compared to the negative control without EsaI (NC). Each error bar represents s.d. (n=6).

c, The rupture of artificial cells through the negative feedback response (**a**) in the artificial cell buffer. Artificial cells containing EsaI are ruptured in significant numbers (Standard one-tail t-test $*P \leq 0.05$) when incubated with bacteria expressing Bac2A (+Bac2A, +EsaI), as compared to negative controls. Each error bar represents s.d. (n=4).

d, The schematic illustrates a negative feedback response between artificial cells and bacteria. AHL produced by EsaI in bacteria is detected by artificial cells. The artificial cells express Bac2A, which penetrates their membrane. Once Bac2A is released in the outside solution, it kills the bacteria. "A" represents EsaI, "S" represents substrates of EsaI, and "R" represents EsaR.

e, CFU of bacteria with the negative feedback response **(d)** at 12 h in H_2O (Blue), PBS (Gray), and artificial cell buffer (Orange). Bacterial densities decrease significantly (Standard two-tail t-test $*P \leq 0.005$) with the feedback response (+EsaI, +Bac2A) compared to their negative controls without either Bac2A, EsaI, or both. Each error bar represents s.d. (n=6).

In the first feedback response, artificial cells containing EsaI are co-incubated with bacteria carrying pIVEX-($P_{T7\text{-}EsaR}$)-Bac2A-2, which expresses Bac2A from the $P_{T7\text{-}EsaR}$ promoter. We only study this feedback response in artificial cell buffer (Figure 5a-c) because the receiver bacteria do not work in H_2O and PBS. Expression of Bac2A in bacteria is inhibited by EsaR but is triggered by AHL from the artificial cells. In the co-incubated system, bacterial density decreases from $4.6x10^9$ to $2.3x10^6$ CFU/ml over 22 hours. In contrast, in a negative control using artificial cells without EsaI, bacterial density increases from $4.5x10^9$ to $6.1x10^9$ CFU/ml over 20 hours. We note that the bacterial density of the negative control decreases slightly in the first 9 hours likely due to

the switch from a nutrient-rich media (LB) with agitation to a media with fewer nutrients and no agitation (Figure 5b). Furthermore, Bac2A is released from bacteria and ruptures 60% of artificial cells after 22 hours. In contrast, in a negative control using artificial cells expressing only GFP, only 10% of artificial cells are ruptured, likely due to the intrinsic instability of artificial cells (Figure 5c). In addition, we test GFP-expressing bacteria as a negative control (Figure S13a) and find that GFP expression is affected by arabinose and AHL (Figure S13b). However, bacterial growth is not affected by arabinose or AHL (Figure S13c). Bacterial growth is also not affected by co-incubation with artificial cells carrying EsaI (Figure S13d).

In the second feedback response, artificial cells containing pIVEX-($P_{T7\text{-}EsaR}$)-Bac2A-1 that expresses Bac2A from the $P_{T7\text{-}EsaR}$ promoter are co-incubated with bacteria carrying pIVEX-(P_{T7})-EsaI (Figure 5d) in H_2O, PBS, and artificial cell buffer. Specifically, bacteria synthesize AHL, which induces the expression of Bac2A in artificial cells. Upon accumulation to a certain level, the Bac2A is released from artificial cells, and then lyses bacteria. There are three possible transport mechanisms of Bac2A in artificial cells: lysis of artificial-cell membranes at high Bac2A concentrations (Figure S12d), diffusion across membranes through lipid flip-flopping[45] or the hemolysin pores. Indeed, when the feedback response is intact, bacterial densities decrease significantly when compared to the negative controls without either EsaI, Bac2A, or both in all three chemical environments. CFU of the bacteria expressing EsaI decreases in all buffers likely due to metabolic burden caused by EsaI (Figure 5e). These results show that the artificial cells are able to both detect and generate a response that kills bacteria regardless of their extracellular chemical context. Taken together, the reduced chemical dependency of artificial cells is established through the parameters described in the first part of this study and demonstrated

through the series of increasingly complex sensing and response genetic circuits successfully tested in different environments.

Conclusion

This work creates a new frontier in using synthetic biology methodology to control artificial cells that interact with each other, as well as with living bacteria in different extracellular chemical contexts. We demonstrate the first negative feedback responses between artificial cells and bacteria in three widely different extracellular chemical contexts, establishing a foundation for more sophisticated two-way feedback responses between artificial cells and bacteria. Buffering synthetic gene networks from their extracellular chemical context is a critical first step toward exploiting the advantages of artificial cells for biotechnological applications. This buffering of synthetic gene networks cannot be achieved using bacteria that can perform protein synthesis in response to quorum sensing molecules in only a rich media. We exemplified how the design, modeling and fine-tuning of genetic modules can lead to the implementation of more complex genetic circuits in artificial cells. Such engineered systems are potentially capable of carrying out a range of autonomous functions, including synchronization of activities, distribution of tasks, and population sensing of environmental factors. We envision that these results will open doors to new mechanisms of coordinating dynamics of engineered vesicles for biomedical applications, as well as new applications of artificial cells for biosensing and therapeutic treatment.

Our work differs from existing work on communication circuits[29-30] of artificial cells in several ways. At the conceptual level, while previous work focuses on demonstrating communication between artificial and living cells, we focus on the robust functioning of artificial cells in three different chemical conditions. The robust functioning of artificial cells is enabled

through the investigation of osmotic balance, crowding density, and membrane composition of artificial cells. At the technical level, our work goes one step beyond existing work by demonstrating that the artificial cells detect bacteria in biofilms through quorum sensing molecules (Figure 4), and they execute feedback response with bacteria through antimicrobial peptides (Figure 5). We note that the feedback response through antimicrobial peptides is a non-trivial technical achievement. The proper functioning of the feedback response requires the artificial cells to detect AHL at the right level, synthesize and release sufficient quantity of peptides at the right time (without being lysed or inhibited by the peptides), and then kill bacteria in three different chemical conditions. The achievement is made possible by the subtle, though critical streamlining of the construction and control of artificial cells. Furthermore, previous work on artificial-cell communication[20, 29] uses the freeze-dried method for constructing artificial cells, which is known for generating liposomes with high heterogeneity [38-39]. Such heterogeneity will likely affect the robustness of artificial cells and diminish the feasibility of implementing the feedback response between artificial and living cells. Furthermore, in contrast to previous work, we demonstrate unilamellarity and relative consistency in the size of artificial cells (10-50μm) through microscopy images (Figure S1). Finally, previous work supplement bacterial lysates in all external environments of artificial cells, and we demonstrate artificial cells that work in H_2O and PBS without supplemented bacterial lysates.

We have adopted a simple design of the biointerface that consists of only phospholipids and cholesterol. The biointerface achieves its function of compartmentalizing the synthetic gene networks while allowing communication between artificial cells and their environments through AHL that freely diffuses through the interface. However, the use of this simple interface that allows chemical communication has a tradeoff: it facilitates the diffusion of small and critical chemical

factors. Due to the tradeoff, even though the artificial cells are able to perform binary signal processing in all three tested external conditions, including sending a quorum sensing signal, receiving a quorum sensing signal, and killing bacteria, their absolute gene expression level is still sensitive (with a lesser degree after our optimization) to their external chemical context. We envision that the incorporation of the active transport of molecules through a less-leaky membrane may help to overcome the tradeoff. For instance, specific membrane transporters can be incorporated to shuttle specific molecules in and out of artificial cells [46]. Similarly, membrane receptors can also be incorporated into the membrane to allow selective transfer of chemical signals that cannot diffuse through the biointerface[47]. Such simple functionalization of the membrane biointerface may further enhance sensing functionality of artificial cells while buffering intracellular reaction networks from their extracellular context. Furthermore, autoregulatory mechanisms may be introduced into artificial cells for maintaining their interior chemical conditions (e.g., crowding density and pH) or concentration of essential molecules (e.g., magnesium, rNTPs, and tRNAs).

Methods

Preparation of artificial cells using the water-in-oil method

Phospholipid (10 mg/ml) and Cholesterol (10 mg/ml) in different ratios were mixed in small glass vials to the total amount of 14 mg and dried overnight under vacuum. For testing different lipid composition, the total concentration is 20 mg/ml, and the molecular ratio between them is as indicated (Figure S1b). 350 µl liquid paraffin was added to dissolve the lipids, and any oxygen was displaced using nitrogen gas. The glass vials were then incubated in a shaker at 37°C overnight. The dissolved lipids remained stable for one month. The interior solution consisted of

whole cell extract (13.5 μl), S12sup (35 μl), 300 ng/μl plasmid (2.5 μl), 2 M sucrose (5.6 μl), 33 nM EsaI (0.5 μl; if needed), and 120 nM mCherry (1 μl; if needed). For preparing artificial cells used for the second feedback response, 10 μl plasmid of 700 ng/μl was included in the interior solution. 30 μl of the interior solution was added to 350 μl liquid paraffin-containing lipids, and the vials were vortexed for 30 s. The water-in-oil emulsion was kept on ice for 10 min and loaded on top of 250 μl of centrifuge buffer (PBS containing 150 mM sucrose) in a 1.5 ml centrifuge tube. Tubes were centrifuged at 3,000g for 20 min at 4°C to pellet the artificial cells, which were then collected using 200 μl pipette tips. The collected artificial cells were washed twice in 300 mM sucrose (for testing communication H_2O), PBS containing 150 mM sucrose (for testing communication in PBS), and dilution buffer (50 mM HEPES, 12 mM Magnesium acetate, 50 mM Potassium gluconate, 80 mM Ammonium acetate, 1 mM DTT, 120 mM sucrose) (for testing communication in artificial cell buffer). Centrifugation at 1,500g for 5 min at 4°C was used when washing artificial cells. Finally, the artificial cells were resuspended with 100 μl H_2O containing 370 mM sucrose and 80 mM NH_4Ac (for testing communication in H_2O), or PBS containing 220 mM sucrose and 80 mM NH_4Ac (for testing communication in PBS), or artificial cell buffer (25 mM HEPES-KOH (pH7.6), 0.6 mM rATP, 0.4 mM rGTP/rCTP/rUTP, 0.085 mg/ml tRNA, 14 μg/ml Folinic acid, 6 mM Magnesium acetate, 25 mM Potassium gluconate, 40 mM Ammonium acetate, 1 mM DTT, 2 mM Spermidine, 33.5 mM Creatine phosphate, 0.32 mM cAMP, 0.75 mM of each 20 amino acids, 200 mM sucrose. For testing the second feedback response, artificial cells were incubated in media containing 200 ng/μl α-hemolysin for 15 min before mixing with bacteria.

One-way communication of artificial cells (Figure 3 & Figure S9-11)

To test artificial cells signaling to bacteria, artificial cells containing EsaI were prepared as described in the section above using components described in Supplementary Materials and Methods, Sections *M.3&M.4*. BL21-AI bacteria containing pAC-EsaR that express EsaR constitutively and pIVEX-($P_{T7\text{-}EsaR}$)-GFP-2 were cultured overnight at 37°C in LB containing 50 μg/ml ampicillin and 50 μg/ml chloramphenicol. 1 μl ($6x10^5$ CFU) of overnight culture was mixed with different volumes of artificial cells (0 μl, 0.001 μl, 0.005 μl, 0.01 μl, 0.05 μl, 0.1 μl, 1 μl). For volumes less than 1 μl, the sample was serial diluted and 1 μl was added. The approximate cell density of 10^6 artificial cells/ml obtained with the ratio EggPC:Chol=1:2 was quantified from microscope images (n=5) using a dilution factor of 1:15 in PBS + 150 mM Sucrose. The cells were identified using ImageJ with the built-in segmentation algorithm. The number was then back-calculated to estimate the cell density per volume. The system was resuspended in 35 μl artificial cell buffer containing 0.002% arabinose, 50 μg/ml ampicillin, and 50 μg/ml chloramphenicol, incubated at 37°C for 5 hours, and analyzed by microscopy and flow cytometry. For negative controls, artificial cells were prepared without EsaI (Figure 3a&b and Figure S9).

To test bacteria signaling to artificial cells, BL21-AI bacteria containing pIVEX-(P_{T7})-EsaI were grown overnight in LB containing 50 μg/ml ampicillin and 0.002% arabinose. Bacteria were washed twice with H_2O before mixing with artificial cells. Artificial cells containing pIVEX-($P_{T7\text{-}EsaR}$)-GFP-1 were prepared as described in the section above using components described in Supplementary Materials and Methods, Sections *M.2&M.4*. 35 μl artificial cells were mixed with different amounts of bacteria (0, $6x10^1$, $6x10^2$,$6x10^3$, $6x10^4$, $6x10^5$, $6x10^6$ CFU) in artificial cell buffer containing 0.002% arabinose, 50 μg/ml ampicillin. For negative controls, different amounts of BL21-AI were incubated with artificial cells at 37°C for 5 hours and analyzed by microscopy and flow cytometry. To test bacteria signaling to artificial cells in H_2O, 370 mM sucrose and 80

mM NH_4Ac were added. To test bacteria signaling to artificial cells in PBS, 220 mM sucrose and 80 mM NH_4Ac were added (Figure 3c&d, Figure S10).

To test sender cells signaling to receiver cells, sender artificial cells containing EsaI and receiver artificial cells containing pIVEX-($P_{T7\text{-}EsaR}$)-GFP-1 were prepared. Different ratios of sender artificial cells and receiver artificial cells (0:15, 0.1:15, 0.2:15, 0.4:15, 0.8:15, 1.5:15, 3:15, 6:15 (v/v)) were mixed, incubated at 37°C for 5 hours, and analyzed by microscopy and flow cytometry. To test sender cells signaling to receiver cells in H_2O, 370 mM sucrose and 80 mM NH_4Ac were added. To test sender cells signaling to receiver cells in PBS, 220 mM sucrose and 80 mM NH_4Ac were added (Figure 3e&f & Figure S11). Sender/receiver ratio refers to solution volume ratio in each condition (Figure 3).

To test artificial cells as biosensor for biofilm, BL21-AI bacteria containing pIVEX-(P_{T7})-EsaI were grown overnight in LB containing 50 μg/ml ampicillin and 0.002% arabinose. To form biofilm, 500 μl overnight culture of bacteria were washed twice with H_2O and mixed with artificial cells containing pIVEX-(PT7-EsaR)-GFP-1 in 35 μl H_2O containing 370 mM sucrose and 80 mM NH_4Ac. Images were taken after incubating at 37°C for 5 hours. For negative control, BL21-AI without plasmid were incubated with artificial cells containing pIVEX-(PT7-EsaR)-GFP-1 (Figure 4).

Negative feedback responses between artificial cells and bacteria (Figure 5 & Figure S12&13)

The first feedback response: Artificial cells containing EsaI were prepared as described above. BL21-AI bacteria with pAC-EsaR and one of the target genes (pIVEX-($P_{T7\text{-}EsaR}$)-Indo-2, or pIVEX-($P_{T7\text{-}EsaR}$)-Bac2A-2, or pIVEX-($P_{T7\text{-}EsaR}$)-GFP-2) were grown overnight at 37°C in LB containing 50 μg/ml ampicillin, 50 μg/ml chloramphenicol and 0.002% arabinose. 1 μl overnight

culture of bacteria was mixed with 35 µl artificial cells in artificial cell buffer containing 50 µg/ml ampicillin, 50 µg/ml chloramphenicol, 0.002% arabinose and 1x proteinase inhibitor cocktail and incubated at 37°C. 3 µl sample was used to measure CFU at 0 h, 3 h, 6 h, 9 h, and 22 h. Another 3 µl sample was used to measure the number of vesicles at 0 h and 22 h using microscopy, 4 replicates were used to obtain an average number of artificial cells at the beginning and the end of the experiment. The average final count for each experiment was subtracted from the average initial number of artificial cells. The resulting numbers were expressed as percentage of ruptured artificial-cells (Figure 5a-c & Figure S12&13).

The second feedback response: Artificial cells containing pIVEX-($P_{T7\text{-}EsaR}$)-Bac2A-1 were prepared as described above. BL21-AI containing pIVEX-(P_{T7})-EsaI was grown overnight at 37°C in LB containing 50 µg/ml ampicillin, and 0.002% arabinose. 0.05 µl overnight culture of bacteria was mixed with 2 µl artificial cells in 20 µl artificial cell buffer containing 50 µg/ml ampicillin, 0.002% arabinose and incubated at 37°C. 3 µl sample was used to measure CFU at 0 h, 12 h. To test the feedback response in H_2O, 370 mM sucrose and 80 mM NH_4Ac were added. To test the feedback response in PBS, 220 mM sucrose and 80 mM NH_4Ac were added (Figure 5d&e).

Supporting Information

Supplementary Results: Quantification and selection of hybrid promoter (R.1.), Mathematical model of artificial cells (R.2.), Construction of feedback responses between bacteria and artificial cells (R.3.), Stability of artificial cells (R.4.). Supplementary Materials and Methods: Materials (M.1.), Plasmid construction and expression control (M.2.), EsaI purification, function analysis and mass spectrometry analysis of N-(3-oxohexanoyl)-L-homoserine lactone (AHL) produced by the purified EsaI (M.3.), Preparation of bacterial extract and S12 supplement (M.4.), Microscopy

and flow cytometry analysis (M.5.), Determination of GFP expression in artificial cells and bacteria from microscopy and flow cytometry results using MATLAB (M.6.), Preparation of giant unilamellar vesicles (GUVs) and treatment with APs (M.7.), Statistical analysis of results (M.8.), Model of communication between artificial cells and bacteria (M.9.). Supplementary figures: Quantifying the yield of artificial cells (Figure S1), Methodology to calculate the %ON using microscope images quantifying GFP intensity at a pixel level (Figure S2), GFP expression in artificial cells with different lipid composition (Figure S3), NH_4Ac is necessary for GFP expression inside artificial cells (Figure S4), GFP expression levels of artificial cells in different environments (Figure S5), Characterization of $P_{T7\text{-}EsaR}$ hybrid promoters (Figure S6), Purified EsaI can synthesize AHL in a whole-cell-extract (Figure S7), Response of bacteria and artificial cells to AHL in artificial cell buffer (Figure S8), Characterization of artificial cells signaling bacteria in artificial cell buffer (Figure S9), Characterization of bacteria signaling artificial cells in H_2O, PBS and artificial cell buffer (Figure S10), Sender artificial cells signaling receiver artificial cells in H_2O, PBS and artificial cell buffer (Figure S11), Measurement of artificial cells and bacteria that express antimicrobial peptides (Figure S12), Negative control for feedback response between cells and bacteria expressing GFP (Figure S13), Primers used in this study (Table S1), Kinetic parameters of the mathematical model (Table S2). Supplementary video: Artificial cells activate GFP expression inside bacteria.

Acknowledgements

We thank Prof. Atul Parikh for sharing organic solvent and functional generator facilities. We appreciate the discussion of the manuscript with Prof. Philip LeDuc, Prof. Atul Parikh, Prof. Robert Smith, and Prof. Erkin Seker. This work is supported by Society-in-Science: Branco-Weiss

Fellowship and NSF-CHE 1808237-0 to C.T. L.E.C-L is supported through a UC MEXUS-CONACYT Doctoral Fellowship.

Author contributions

Y.D. and C.T. designed the communication circuits and artificial cells. Y.D. constructed the circuits and artificial cells. Y.D. and L.E.C-LL. tested the communication between artificial cells and bacteria in different chemical contexts. E.M. and C.T. developed the computational models. E.M. tested AHL production rate. M.M tested the yield of artificial cells using different lipids. All authors wrote the manuscript.

Competing financial interests

The authors declare no competing financial interests.

References

1. Cardinale, S.; Arkin, A. P., Contextualizing Context for Synthetic Biology--Identifying Causes of Failure of Synthetic Biological Systems. *Biotechnol J* **2012,** *7* (7), 856-866.
2. Scott, M.; Gunderson, C. W.; Mateescu, E. M.; Zhang, Z.; Hwa, T., Interdependence of Cell Growth and Gene Expression: Origins and Consequences. *Science* **2010,** *330* (6007), 1099-1102.
3. Tan, C.; Marguet, P.; You, L., Emergent Bistability by a Growth-Modulating Positive Feedback Circuit. *Nat Chem Biol* **2009,** *5* (11), 842-848.
4. Chavez, M.; Ho, J.; Tan, C., Reproducibility of High-Throughput Plate-Reader Experiments in Synthetic biology. *ACS Synth Biol* **2017**, 6 (2), 375-380.
5. Del Vecchio, D.; Ninfa, A. J.; Sontag, E. D., Modular Cell Biology: Retroactivity and Insulation. *Mol Syst Biol* **2008,** *4*, 161.
6. Lou, C.; Stanton, B.; Chen, Y. J.; Munsky, B.; Voigt, C. A., Ribozyme-Based Insulator Parts Buffer Synthetic Circuits from Genetic Context. *Nat Biotechnol* **2012,** *30* (11), 1137-1142.
7. Mishra, D.; Rivera, P. M.; Lin, A.; Del Vecchio, D.; Weiss, R., A Load Driver Device for Engineering Modularity in Biological Networks. *Nat Biotechnol* **2014,** *32* (12), 1268-1275.
8. Hussain, F.; Gupta, C.; Hirning, A. J.; Ott, W.; Matthews, K. S.; Josic, K.; Bennett, M. R., Engineered Temperature Compensation in a Synthetic Genetic Clock. *Proc Natl Acad Sci U S A* **2014,** *111* (3), 972-977.
9. Tamsir, A.; Tabor, J. J.; Voigt, C. A., Robust Multicellular Computing using Genetically Encoded NOR Gates and Chemical 'Wires'. *Nature* **2011,** *469* (7329), 212-215.
10. Szostak, J. W.; Bartel, D. P.; Luisi, P. L., Synthesizing Life. *Nature* **2001,** *409* (6818), 387-390.

11. Noireaux, V.; Libchaber, A., A Vesicle Bioreactor as a Step Toward an Artificial Cell Assembly. *Proc Natl Acad Sci U S A* **2004,** *101* (51), 17669-17674.
12. Mansy, S. S.; Schrum, J. P.; Krishnamurthy, M.; Tobe, S.; Treco, D. A.; Szostak, J. W., Template-Directed Synthesis of a Genetic Polymer in a Model Protocell. *Nature* **2008,** *454* (7200), 122-125.
13. Gardner, P. M.; Winzer, K.; Davis, B. G., Sugar Synthesis in a Protocellular Model Leads to a Cell Signalling Response in Bacteria. *Nat Chem* **2009,** *1* (5), 377-383.
14. Kolmakov, G. V.; Yashin, V. V.; Levitan, S. P.; Balazs, A. C., Designing Communicating Colonies of Biomimetic Microcapsules. *Proc Natl Acad Sci U S A* **2010,** *107* (28), 12417-12422.
15. Kurihara, K.; Tamura, M.; Shohda, K.; Toyota, T.; Suzuki, K.; Sugawara, T., Self-Reproduction of Supramolecular Giant Vesicles Combined With the Amplification of Encapsulated DNA. *Nat Chem* **2011,** *3* (10), 775-781.
16. Dzieciol, A. J.; Mann, S., Designs for Life: Protocell Models in the Laboratory. *Chem Soc Rev* **2012,** *41* (1), 79-85.
17. Tan, C.; Saurabh, S.; Bruchez, M. P.; Schwartz, R.; Leduc, P., Molecular Crowding Shapes Gene Expression in Synthetic Cellular Nanosystems. *Nat Nanotechnol* **2013,** *8* (8), 602-608.
18. Kobori, S.; Ichihashi, N.; Kazuta, Y.; Yomo, T., A Controllable Gene Expression System in Liposomes that Includes a Positive Feedback Loop. *Mol Biosyst* **2013,** *9* (6), 1282-1285.
19. Black, R. A.; Blosser, M. C.; Stottrup, B. L.; Tavakley, R.; Deamer, D. W.; Keller, S. L., Nucleobases Bind to and Stabilize Aggregates of a Prebiotic Amphiphile, Providing a Viable Mechanism for the Emergence of Protocells. *Proc Natl Acad Sci U S A* **2013,** *110* (33), 13272-13276.
20. Lentini, R.; Santero, S. P.; Chizzolini, F.; Cecchi, D.; Fontana, J.; Marchioretto, M.; Del Bianco, C.; Terrell, J. L.; Spencer, A. C.; Martini, L.; Forlin, M.; Assfalg, M.; Dalla Serra, M.; Bentley, W. E.; Mansy, S. S., Integrating Artificial with Natural Cells to Translate Chemical Messages that Direct E. coli Behaviour. *Nature communications* **2014,** *5*, 4012.
21. Weitz, M.; Kim, J.; Kapsner, K.; Winfree, E.; Franco, E.; Simmel, F. C., Diversity in the Dynamical Behaviour of a CompArtmentalized Programmable Biochemical Sscillator. *Nat Chem* **2014,** *6* (4), 295-302.
22. Walde, P.; Umakoshi, H.; Stano, P.; Mavelli, F., Emergent Properties Arising from the Assembly of Amphiphiles. Artificial Vesicle Membranes as ReactionPromoters and Regulators. *Chem Commun (Camb)* **2014,** *50* (71), 10177-10197.
23. Chou, L. Y.; Zagorovsky, K.; Chan, W. C., DNA Assembly of Nanoparticle Superstructures for Controlled Biological Delivery and Elimination. *Nat Nanotechnol* **2014,** *9* (2), 148-155.
24. Studart, A. R., Biologically Inspired Dynamic Material Systems. *Angew Chem Int Ed Engl* **2015,** *54* (11), 3400-3416.
25. Blain, J. C.; Szostak, J. W., Progress Toward Synthetic cells. *Annu Rev Biochem* **2014,** *83*, 615-640.
26. van Roekel, H. W.; Rosier, B. J.; Meijer, L. H.; Hilbers, P. A.; Markvoort, A. J.; Huck, W. T.; de Greef, T. F., Programmable Chemical Reaction Networks: Emulating Regulatory Functions in Living Cells Using a Bottom-Up Approach. *Chem Soc Rev* **2015,** *44* (21), 7465-7483.
27. Xu, C.; Hu, S.; Chen, X., Artificial Cells: From Basic Science to Applications. *Mater Today (Kidlington)* **2016,** *19* (9), 516-532.
28. Buddingh, B. C.; van Hest, J. C. M., Artificial Cells: Synthetic Compartments with Life-like Functionality and Adaptivity. *Acc Chem Res* **2017,** *50* (4), 769-777.
29. Lentini, R.; Martin, N. Y.; Forlin, M.; Belmonte, L.; Fontana, J.; Cornella, M.; Martini, L.; Tamburini, S.; Bentley, W. E.; Jousson, O.; Mansy, S. S., Two-Way Chemical Communication Between Artificial and Natural Cells. *ACS Cent Sci* **2017,** *3* (2), 117-123.
30. Schwarz-Schilling, M.; Aufinger, L.; Muckl, A.; Simmel, F. C., Chemical Communication Between Bacteria and Cell-Free Gene Expression Systems within Linear Chains of Emulsion Droplets. *Integr Biol-Uk* **2016,** *8* (4), 564-570.
31. Adamala, K. P.; Martin-Alarcon, D. A.; Guthrie-Honea, K. R.; Boyden, E. S., Engineering Genetic Circuit Interactions within and between Synthetic Minimal Cells. *Nature Chemistry* **2017**, 9, 431-439.
32. Qiao, Y.; Li, M.; Booth, R.; Mann, S., Predatory Behaviour in Synthetic Protocell Communities. *Nat Chem* **2017,** *9* (2), 110-119.
33. Krinsky, N.; Kaduri, M.; Zinger, A.; Shainsky-Roitman, J.; Goldfeder, M.; Benhar, I.; Hershkovitz, D.; Schroeder, A., Synthetic Cells Synthesize Therapeutic Proteins inside Tumors. *Adv Healthc Mater* **2018**, 7, 1701163.

34. Lee, K. Y.; Park, S. J.; Lee, K. A.; Kim, S. H.; Kim, H.; Meroz, Y.; Mahadevan, L.; Jung, K. H.; Ahn, T. K.; Parker, K. K.; Shin, K., Photosynthetic Artificial Organelles Sustain and Control ATP-Dependent Reactions in a Protocellular System. *Nat Biotechnol* **2018,** 36, 530-535.
35. Gardner, P. M.; Winzer, K.; Davis, B. G., Sugar Synthesis in a Protocellular Model Leads to a Cell Signalling Response in Bacteria. *Nature Chemistry* **2009,** *1*, 377-383.
36. Leduc, P. R.; Wong, M. S.; Ferreira, P. M.; Groff, R. E.; Haslinger, K.; Koonce, M. P.; Lee, W. Y.; Love, J. C.; McCammon, J. A.; Monteiro-Riviere, N. A.; Rotello, V. M.; Rubloff, G. W.; Westervelt, R.; Yoda, M., Towards an in vivo Biologically Inspired Nanofactory. *Nat Nanotechnol* **2007,** *2* (1), 3-7.
37. Morris, E.; Chavez, M.; Tan, C., Dynamic Biomaterials: Toward Engineering Autonomous Feedback. *Curr Opin Biotechnol* **2016,** *39*, 97-104.
38. Hope, M. J.; Bally, M. B.; Webb, G.; Cullis, P. R., Production of Large Unilamellar Vesicles by a Rapid Extrusion Procedure: Characterization of Size Distribution, Trapped Volume and Ability to Maintain a Membrane Potential. *Biochim Biophys Acta* **1985,** *812* (1), 55-65.
39. Martino, C.; deMello, A. J., Droplet-Based Microfluidics for Artificial Cell Generation: a Brief Review. *Interface Focus* **2016,** *6* (4), 20160011.
40. Raffy, S.; Teissie, J., Control of Lipid Membrane Stability by Cholesterol Content. *Biophys J* **1999,** *76* (4), 2072-2080.
41. Shong, J.; Huang, Y. M.; Bystroff, C.; Collins, C. H., Directed Evolution of the Quorum-Sensing Regulator EsaR for Increased Signal Sensitivity. *ACS Chem Biol* **2013,** *8* (4), 789-795.
42. Elani, Y.; Law, R. V.; Ces, O., Vesicle-Based Artificial Cells as Chemical Microreactors with Spatially Segregated Reaction Pathways. *Nature communications* **2014,** *5*, 5305.
43. Stewart, P. S.; Franklin, M. J., Physiological Heterogeneity in Biofilms. *Nat Rev Microbiol* **2008,** *6* (3), 199-210.
44. Wu, M.; Hancock, R. E., Improved Derivatives of Bactenecin, a Cyclic Dodecameric Antimicrobial Cationic Peptide. *Antimicrob Agents Chemother* **1999,** *43* (5), 1274-1276.
45. Zhang, L.; Rozek, A.; Hancock, R. E., Interaction of Cationic Antimicrobial Peptides with Model Membranes. *J Biol Chem* **2001,** *276* (38), 35714-35722.
46. International Transporter, C.; Giacomini, K. M.; Huang, S. M.; Tweedie, D. J.; Benet, L. Z.; Brouwer, K. L.; Chu, X.; Dahlin, A.; Evers, R.; Fischer, V.; Hillgren, K. M.; Hoffmaster, K. A.; Ishikawa, T.; Keppler, D.; Kim, R. B.; Lee, C. A.; Niemi, M.; Polli, J. W.; Sugiyama, Y.; Swaan, P. W.; Ware, J. A.; Wright, S. H.; Yee, S. W.; Zamek-Gliszczynski, M. J.; Zhang, L., Membrane Transporters in Drug Development. *Nat Rev Drug Discov* **2010,** *9* (3), 215-236.
47. Cuatrecasas, P., Membrane receptors. *Annu Rev Biochem* **1974,** *43* (0), 169-214.